Chemical Engineering Journal 165 (2010) 958–965

Contents lists available at ScienceDirect

Chemical Engineering Journal

journal homepage: www.elsevier.com/locate/cej

Effect of water content on growth and optical properties of ZnO nanoparticles generated in binary solvent mixtures by micro-continuous flow synthesis

S. Li*, S. Meierott, J.M. Köhler

Ilmenau University of Technology, Institute for Micro and Nanotechnologies, Dept. of Physical Chemistry and Micro Reaction Technology, Weimarer Str. 32, D-98693 Ilmenau, Germany

ARTICLE INFO

Article history:
Received 22 April 2010
Received in revised form 27 July 2010
Accepted 16 August 2010

Keywords:
Zinc oxide
Nanoparticles
Micro-reactor
Segmented flow
Micro-continuous flow
Optical property

ABSTRACT

The technique of micro-segmented flow was used for continuous synthesis of ZnO nanoparticles. In the experimental setup, a static micro-mixer was applied for mixing the precursor solutions at room temperature. Then micro-fluid segments were formed by injecting the mixture into a stream of carrier. The formation of ZnO particles started after the fluid segments were led in PFTE tube coils inside a thermostat at enhanced temperature. Two different experimental conditions were applied to prepare ZnO nanoparticles, where $Zn(Ac)_2$ and NaOH in ethylene glycol (EG) were mixed with water (at lower pH, pH = 12.3, 100 °C) or water/EG mixing solvent (higher pH, pH = 12.7, 90 °C) to achieve varied water content in the final mixture solution. The formation of homogeneous quasi-spherical particles at lower water content was proven by TEM and SEM. In the first case, a stronger dependence of particle size on water content (diameters between 18 and 436 nm in a water content range between 15 v% and 90 v%) was observed. In the second case, a lower solvent effect (diameters between 33 nm and 168 nm in a water content range between 15 and 60 v%) was observed. The strong effect of water content on the size of the resulting particles was also reflected by the optical properties of the nanoparticles. So, the water-to-solvent-ratio can be used for tuning the optical absorption of ZnO nanoparticles. The characteristic UV absorption peak was shifted between 317 nm and 373 nm by an enhancement of the water content from 15 v% to 90 v% if the particle formation was initiated by mixing $Zn(Ac)_2$ and NaOH in ethylenglycol with water.

1. Introduction

During the past few years, nanocrystals of zinc oxide have attracted a lot of interest due to their potential applications, such as solar cells [1–3], photocatalysts [4,5], luminescent materials [6,7], gas sensors [8–10] and so on. Different technologies have been developed to synthesize ZnO nanocrystals with different shapes and sizes, including hydrothermal synthesis [11,12], sol–gel method [13–15], thermal decomposition [16,17], microwave irradiation method [18–20], chemical vapor deposition [21,22], and continuous flow techniques [23,24]. Among these methods, polyol-mediated synthesis [25–28] is well suited for the preparation of nanoparticles with a narrow size distribution and high crystalline quality. This method is realized by dissolving a suitable metal precursor in polyol solvent, such as ethylene glycol, diethylene glycol and glycerol, and then heating at high temperature. The solvent can act as a stabilizer and limit particle growth and agglomeration after heating. It is comparably easy to perform and has been applied to synthesis different metal [29–31] and metal oxide nanoparticles [25,26,32,33].

Recently, the micro-fluid segment technique has been under investigation for a lot of chemical [34–39] and biological [35,40,41] applications. In this technology, fluid segments are embedded in a non-miscible carrier liquid and plug-like transported. The ability of formation of highly regular segments and segment distances ensure constant process conditions and a very narrow distribution of residence time and temperature changes for the whole reaction volume. In addition, transported induced segment-internal convection can enhance fast mixing and heat transfer. Therefore, equal reaction conditions in all segments can be realized.

To the best of our knowledge, there have been no reports about the application of micro-segmented flow for the formation of ZnO nanocrystals in ethylene glycol. This method offers several advantages compared to other ZnO synthesis. It would be very interesting for preparation of other nanomaterials. Here, the continuous-flow synthesis of ZnO nanoparticles was investigated.

2. Experimental

2.1. Experimental arrangement and devices

The synthesis of ZnO particles was realized by following multi-step micro-continuous-flow process:

* Corresponding author.
E-mail address: shuning.li@tu-ilmenau.de (S. Li).

1385-8947/$ – see front matter © 2010 Elsevier B.V. All rights reserved.
doi:10.1016/j.cej.2010.08.033

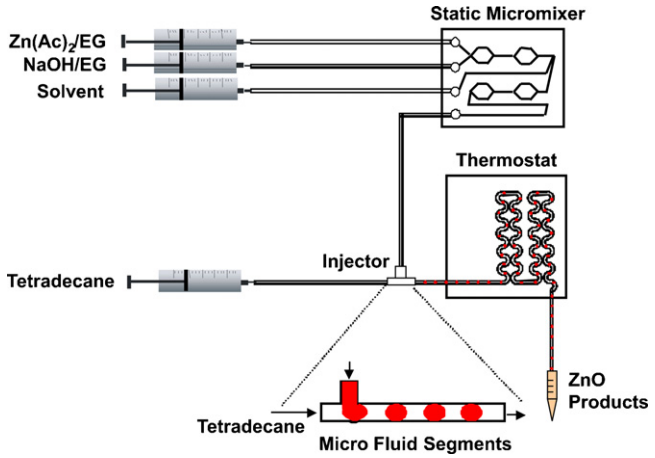

Fig. 1. Experimental arrangement.

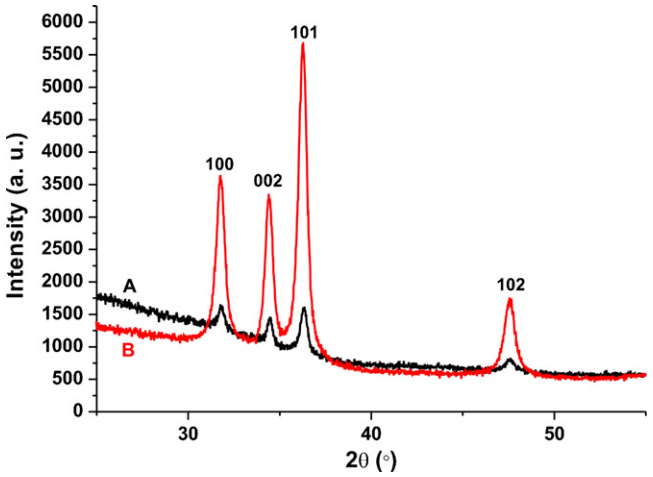

Fig. 2. XRD patterns of as-prepared ZnO particles. (A) water content: 50 v% (condition A); (B) water content: 30 v% (condition B).

(1) Homogeneous mixing of ethylene glycol solution of NaOH and $Zn(CH_3COO)_2$ as well as solvent by a static micro-mixer. The volume of the static micro-mixer was 10 μL and the mixing time was calculated to be 0.3 s and 4 s for condition A and B, respectively.
(2) Formation of segmented flow by injection of the reaction mixture into a carrier stream of tetradecane.
(3) Reaction initiation by fast heating.
(4) Particle growth in a final residence loop (ID: 1.0 mm; L: 1.0 m) inside the thermostat. The residence time was 9 s and 72 s for condition A and B, respectively.

The experimental set-up (Fig. 1) was composed of four PC-controlled syringe pumps delivering the fluids at a constant flow rate, a static micro-static micro-mixer (Statmix 6, IPHT Jena [42]) used for mixing of reactants, an injector for segment formation and PTFE tube coil placed inside a thermostat allowing the application of temperatures up to 150 °C. A micro-flow-through photometer (LED peak at 610 nm, Agilent, Santa Clara CA, United States) mounted between the injector and thermostat was applied to detect the segments.

2.2. Characterization

The measurement of pH was realised by a cyberscan PC 510 (EUTECH instruments, www.eutechinst.com) pH-electrode. TEM investigation was carried out on Philips Tecnai S 20 transition electron microscope with an accelerating voltage of 200 kV. For SEM measurement (Hitachi S-4800 FE-SEM), the product solutions were applied on Si chips, particles were adsorbed and then rinsed with water and ethanol. The average diameter and size distribution of ZnO particles was determined by measuring at least 100 randomly selected particles by use of TEM and SEM images at a magnification factor of 100,000×. Optical spectra of ZnO particles were recorded by a UV/vis spectrophotometer (Specord 200, Analytik Jena, Germany) with scanning speed of 10 nm/s over a scanning wavelength range of 200–800 nm; the samples were dispersed in deionised water. X-ray diffraction (XRD) analysis was carried out on a Siemens D-5000 X-ray diffractometer using Cu-Kα radiation (λ = 0.15478 nm) with step size of 0.02°. Thermogravimetric analysis was recorded using Netzsch STA 409 EP from 30 °C to 750 °C with a heating rate of 10 °C/min under flowing air.

2.3. Chemicals

Zinc acetate dihydrate (Acros Organics, USA, purity: 98%), sodium hydroxide (Merck, Germany, purity: 99%), ethylene glycol (Acros Organics, USA, purity: 99.97%) and tetradecane (Acros Organics, USA, purity: 99%) were used as received. Deionised water (Aqua purificator G 7795, Miele, Germany) was used for all preparations.

3. Results and discussions

In ZnO micro- and nanoparticle synthesis, there are a lot of experimental parameters which can influence resulting particle size and shape, such as temperature, solvent and reaction time as well as concentration of precursors and water. However, in this paper, we focussed on the investigation of the effect of water con-

Table 1
Experimental conditions.

Experimental condition		$Zn(Ac)_2$ in EG	NaOH in EG	Solvent	Tetradecane	T	H_2O content	Products
A	Conc. (M)	0.02	0.2	H_2O	3000	100 °C		
	Flow rate (μL/min)	850	850	300			15 v%	Fig. 3(A–C)
		750	750	500			25 v%	Fig. 3(D–F)
		650	650	700			35 v%	Fig. 3(G–I)
		500	500	1000			50 v%	Fig. 3(J–L)
		250	250	1500			75 v%	Fig. 3(M–O)
		100	100	1800			90 v%	Fig. 3(P–R)
B	Conc. (M)	0.05	1	EG/H_2O	500	90 °C		
	Flow rate (μL/min)	30	30	90			15 v%	Fig. 6(A and B)
							25 v%	Fig. 6(C and D)
							30 v%	Fig. 6(E and F)
							45 v%	Fig. 6(G and H)
							60 v%	Fig. 6(I and J)

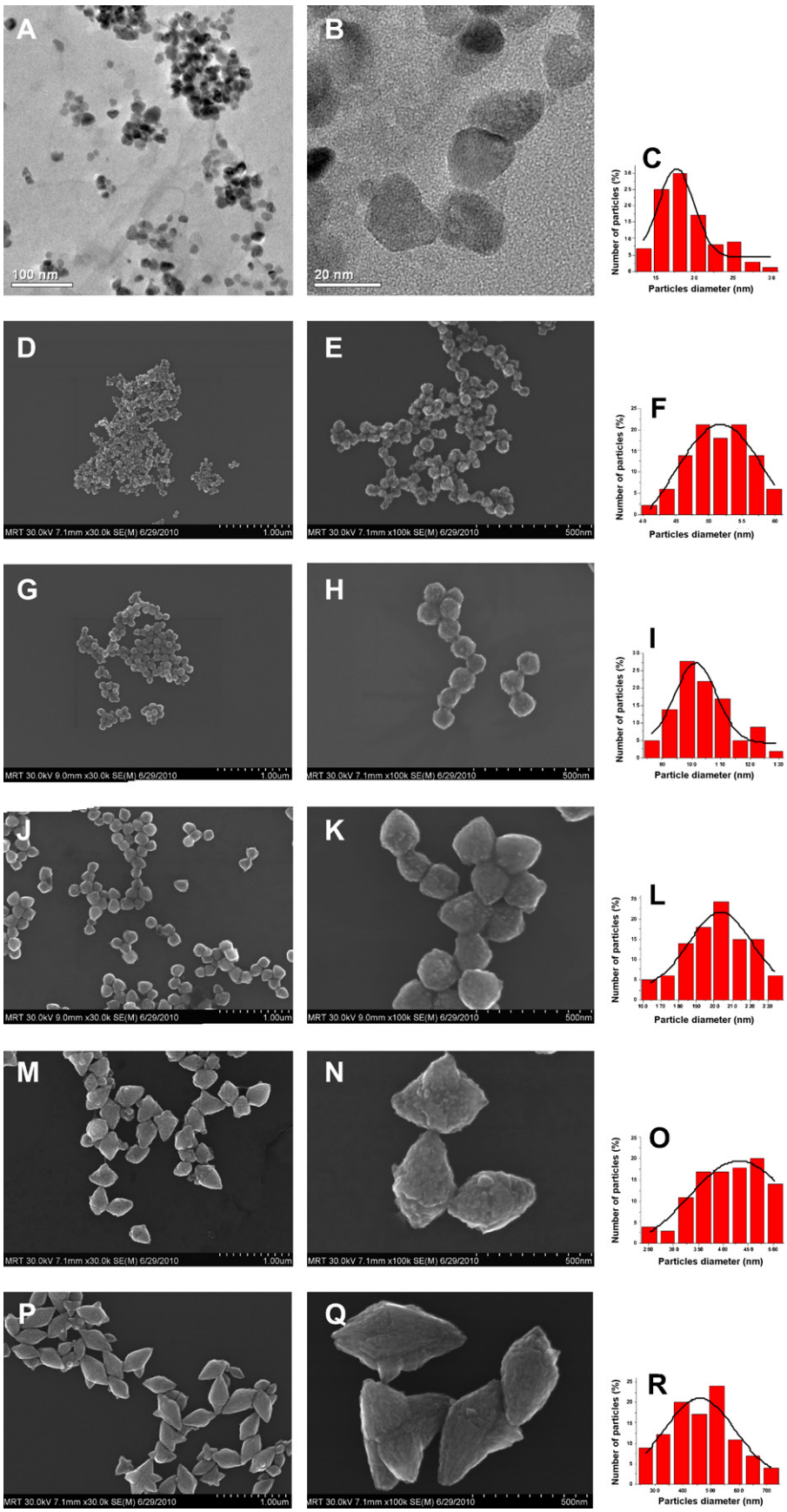

Fig. 3. Effect of water content on shape, size and size distribution of ZnO particles under experimental condition A (0.02 M $Zn(Ac)_2$, 0.2 M NaOH, 100 °C, 5000 μL/min) demonstrated by TEM and SEM images: (A, B, C) 15 v%; (D, E, F) 25 v%; (G, H, I) 35 v%; (J, K, L) 50 v%; (M, N, O) 75 v%; (P, Q, R) 90 v%.

tent in binary solvent mixtures on the characteristics of obtained particles under two different experimental conditions by micro-flow-through synthesis. Preliminary investigations of the effect of solvents on the formation of ZnO micro- and nanoparticles by hydrothermal synthesis had shown qualitatively the dominance of water on the quality of the formed particles. In particular, the transition between more compact and star-like or flower-like particles was strongly effected by the presence of water. Therefore, here the effect of water in the hydrothermal synthesis of zinc oxide in ethylene glycol by precipitation at high pH and elevated temperature was studied.

Despite of the higher probability of wall interactions, micro-reaction technology is an interesting alternative to batch synthesis [25–28] for the generation of nanoparticles. The hydrothermal synthesis can profit from fast heat and mass transfer which can be realized under micro-flow conditions. It could be expected that the homogeneity of ZnO particles can be improved if a micro-continuous flow process is applied. In contrast to homogenous fluids, the application of micro-segmented flow is particular promising for ZnO nanoparticle synthesis if the wall surface is hydrophobic and shows good wetting conditions for the inert carrier liquid and a high contact angle with the reaction mixture. In this case, the interaction between reactants and wall can be reduced

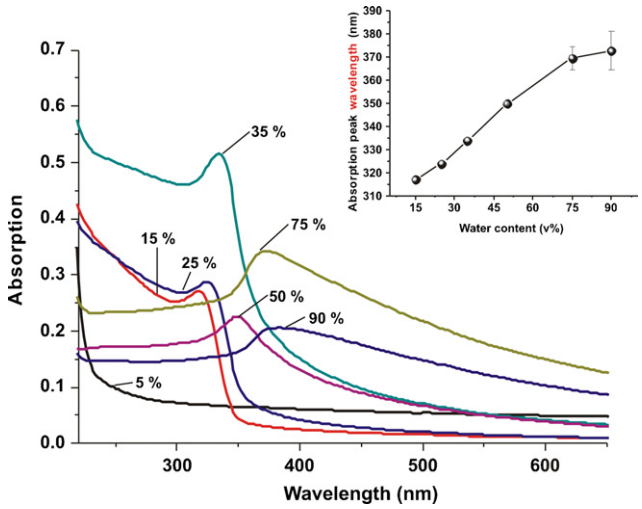

Fig. 4. UV–vis spectra of ZnO particles obtained with different water contents under experimental condition A (0.02 M $Zn(Ac)_2$, 0.2 M NaOH, 100 °C, 5000 μL/min). Inset shows the absorption peaks of ZnO particles in the presence of different water contents.

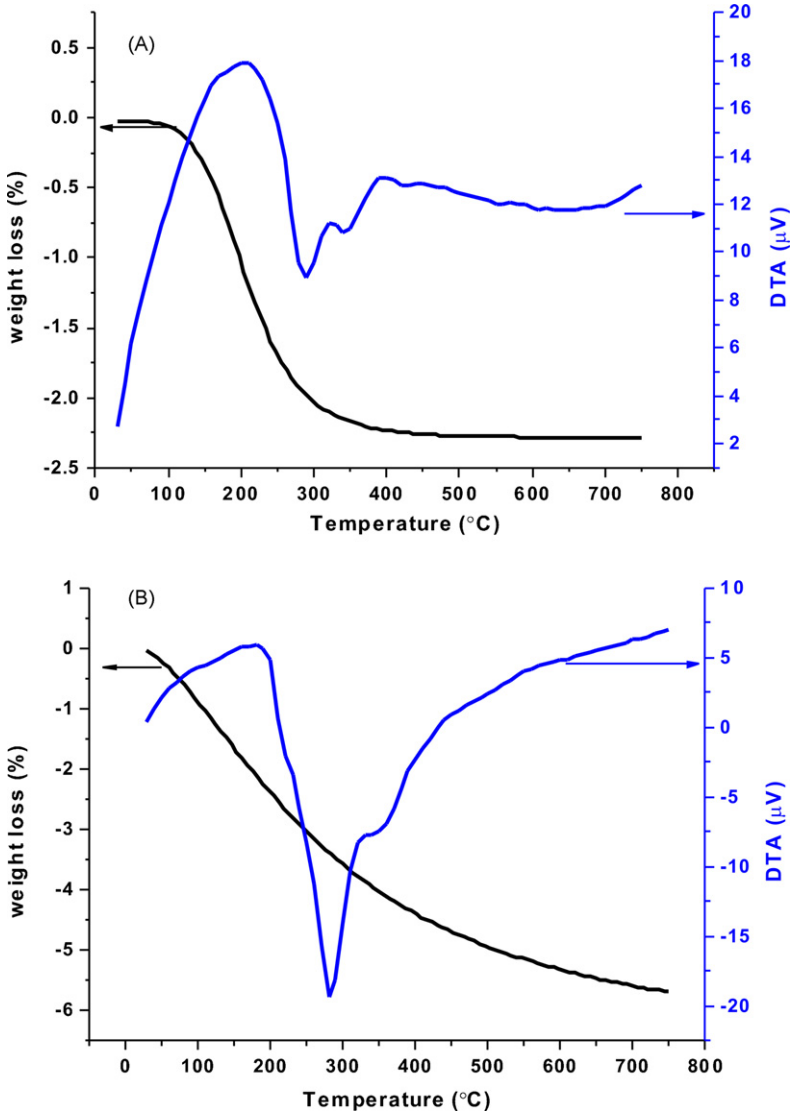

Fig. 5. TG–DTA curves of ZnO products under condition A: (A) water content: 50 v%; (B) water content: 35 v%.

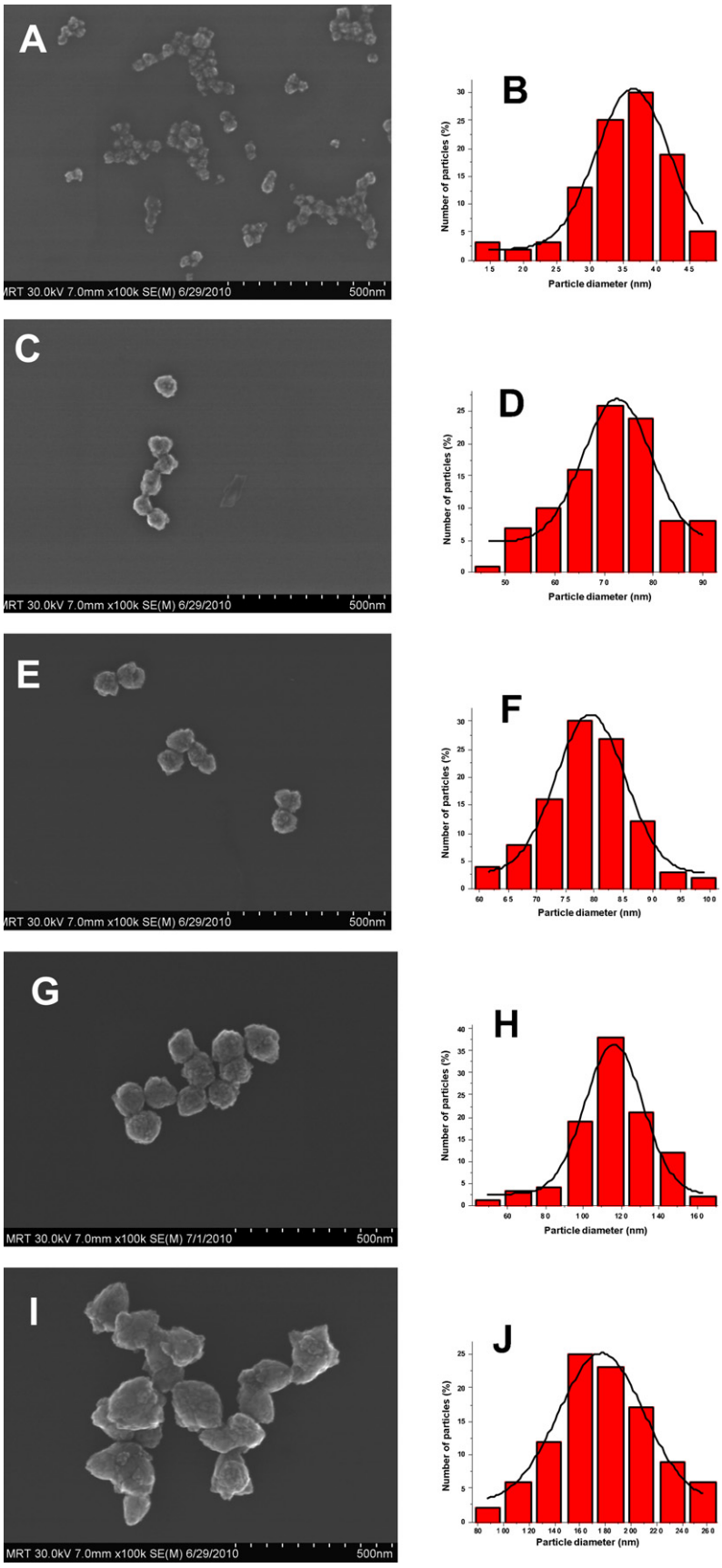

Fig. 6. Effect of water content on shape, size and size distribution of ZnO particles under experimental condition B (0.05 M $Zn(Ac)_2$, 1 M NaOH, 90 °C, 650 μL/min) demonstrated by SEM images: (A, B) 15 v%; (C, D) 25 v%; (E, F) 30 v%; (G, H) 45 v%; (I, J) 60 v%.

drastically and the initiation of nucleation or the deposition of particles at the wall surface can be suppressed [43]. In addition, the segment-interval convection caused by the motion of fluid segments can be used for acceleration of heat transfer and enhancing fast mixing [38,44,45]. This process is intensified by increasing flow rate, which would lead to the reduction of reaction time.

Table 1 presented the details of the used experimental parameters. For experimental condition A, the formation of ZnO particles was carried out at higher total flow rate (5000 μL/min) and enhanced temperature (100 °C) as well as lower concentration ratio of NaOH/$Zn(CH_3COO)_2$ (10/1). Different water contents from 5 v% to 90 v% were realized by adjusting the flow rates of reactant solutions. In comparison, for experimental condition B, it occurred at lower total flow rate (650 μL/min) and reduced temperature (90 °C) as well as higher concentration ratio of NaOH/$Zn(CH_3COO)_2$ (20/1). The segment size for condition A and B was about 0.77 μL or 1.1 μL, respectively. By changing the solvent ratio of water/EG, varied water contents were achieved while the flow rate of each reactant always keeps constant during the synthesis procedure.

Fig. 2 shows the XRD patterns of two typical as-prepared ZnO products. All the diffraction peaks in Fig. 2 can be exactly indexed to the hexagonal wurtzite ZnO with lattice structure of $a = 3.25$ Å and $c = 5.21$ Å ($c/a = 1.60$), which was in good agreement with the values in the standard card (JCPDS card 36-1451). In addition, no characteristic diffraction peaks from other phases or impurities were found.

From the TEM and SEM images from experimental condition A (Fig. 3), it can be seen that the shape and size of the obtained particles strongly depend on water content in the system. When water content was below 35 v%, homogeneous quasi-spherical ZnO nanoparticles (Fig. 3A, B, D, E, G and H) were synthesized. At the same time, average particle size increased from 18 nm to 102 nm if water content enhanced from 15 v% to 35 v%. Size distribution graphs of these particles are shown in Fig. 3C, F, I and L. Furthermore, the particle shape shifted from nut-like (Fig. 3J and K) to ellipsoidal (Fig. 3M, N, P and Q) when water content increased from 50 v% to 90 v%. Meanwhile, particle size enhanced significantly from 196 nm to 436 nm and particles size distribution became broad (Fig. 3L, O and R).

Besides the particles size, the effect of water content also influenced the UV/vis spectra of the products. From Fig. 4, it can be observed that the absorption peak of the obtained ZnO particles changed from 317 nm to 373 nm when water content increasing from 15 v% to 90 v%. In particular, if water content was 5 v%, there was no absorption peak since no precipitation occurred. From the inset graph in Fig. 4, we can clearly observe the increase of the wavelength of absorption peaks with enhancing water contents, which was associated with particle growth [46]. It is already reported that the dependence of particles size on the optical absorption spectra can be determined by using the effective mass model; details of the calculation can be found in Ref. [47,48].

These results are consistent with the results of polyol-mediated synthesis [32], where water plays an important role in determining the particle shape and size since water can induce hydrolysis and condensation reactions for the Zn precursor [26]. At lower water content, ethylene glycol as a chelating agent, can adsorb on the surface of the nucleus, thus limiting the particle growth and avoiding agglomeration. Therefore, quasi-spherical particles with homogeneous size distribution were obtained when water content was below 35 v%. If water content was enlarged, sufficient water was present to hydrolyze the Zn complexes and enhanced growth rate was expected. Therefore, the resulting particles became larger and inhomogeneous due to a lower concentration of ethylene glycol, the assumed complexing agent that inhibits particle growth and aggregation.

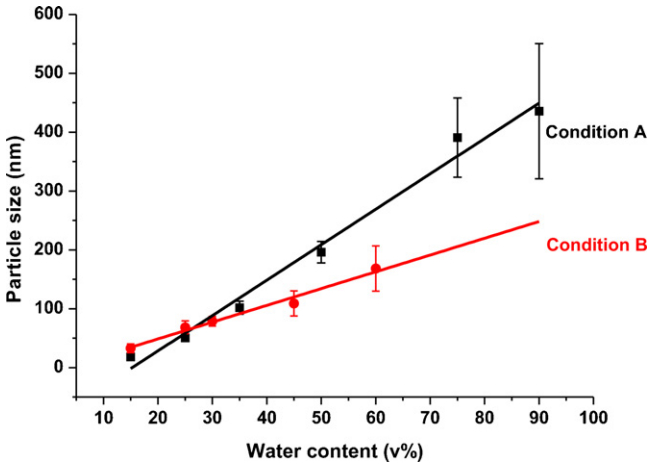

Fig. 7. Comparison of effect of water content on particle size for experimental condition A (0.02 M $Zn(Ac)_2$, 0.2 M NaOH, 100 °C, 5000 μL/min) and B (0.05 M $Zn(Ac)_2$, 1 M NaOH, 90 °C, 650 μL/min).

In order to investigate composition of obtained ZnO particles, we carried out TG–DTA measurements for two samples with water content of 35 v% and 50 v% shown in Fig. 5. In Fig. 5A, two weight losses were observed at about 30–200 °C and 200–400 °C in the TG curve. The first weight loss was due to the removal of physically absorbed water. The second weight loss can be attributed to the decomposition of ethylene glycol on ZnO particles. In the TG curve of Fig. 5B, the first weight loss between 30 °C and 300 °C can be ascribed to the departure of absorbed water and combustion of part of adsorbed ethylene glycol. The second weight loss between 300 °C and 750 °C could be caused by burnout of strongly bounded ethylene glycol since the lower water content under this condition. These results have been already observed and confirmed by other authors [49]. On both of the DTA curves, two exothermic peaks were observed at about 280 °C and 340 °C, respectively. These peaks were associated with decomposition of the organics. The total weight loss for these two measurements was 2.2% with water content of 50 v% and 5.5 v% with water content of 35 v%, respectively. It supported our assumption mentioned before that particle size can be suppressed at lower water content since higher content of ethylene glycol can adsorb on the surface of the particles.

On the other hand, under experimental condition B, quasi-spherical ZnO nanoparticles were obtained for water contents between 15 v% and 45 v%. Dakhlaoui et al. [49] and Wang et al. [50] also observed that at higher alkaline ratio, the particle appeared in spherical shape. SEM images under this condition are shown in Fig. 6, which demonstrated that particle size slightly increased with enhancing water content. Size distribution graphs (Fig. 6B, D, F, H, J) showed the obtained particles had narrow size distribution. Fig. 7 compared the effect of water content on particle size under both experimental conditions. It indicated that obtained particle size was strongly dependent on water content in binary solvent mixtures. Furthermore, the effect of water content on particle size at experimental condition A was more noticeable than condition B. UV/vis absorption spectra for ZnO products under condition B are shown in Fig. 8. All spectra are marked by the characteristic peak in the UV range (at about 340 nm). But, the peak shift with water content is much smaller than in the case of conditions A. In addition, the shift of absorption in the longer wavelength range is considerably reduced. The insert graph in Fig. 8 revealed the absorption peak wavelength of obtained ZnO particles as a function of water content. It was similar to the insert graph in Fig. 4. Fig. 9 investigated the effect of water content on absorption peak wavelength under condition A and B. It matched well with Fig. 7 since absorption peak wavelength was dependent on particle size.

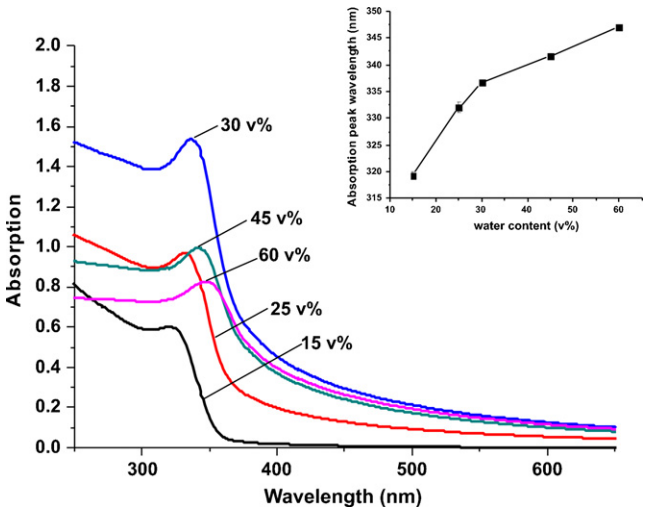

Fig. 8. UV–vis spectra of ZnO particles obtained with different water contents under experimental condition B (0.05 M $Zn(Ac)_2$, 1 M NaOH, 90 °C, 650 μL/min). Inset shows the absorption peak wavelength as a function of water contents.

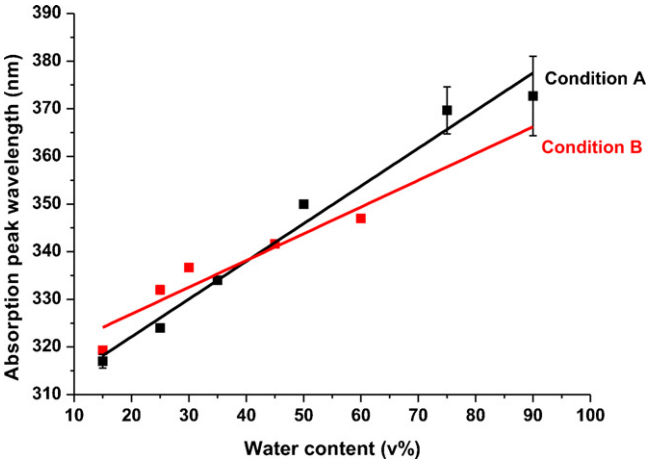

Fig. 9. Comparison of effect of water content on absorption peak wavelength for experimental condition A (0.02 M $Zn(Ac)_2$, 0.2 M NaOH, 100 °C, 5000 μL/min) and B (0.05 M $Zn(Ac)_2$, 1 M NaOH, 90 °C, 650 μL/min).

4. Conclusions

In this work, it could be shown that the preparation of high quality ZnO nanoparticle by using $Zn(Ac)_2$ and NaOH as reactants in binary solvents of water and ethylene glycol is possible in a hydrothermal micro-continuous flow synthesis. By changing the water content in reactant solutions from 5 v% to 90 v%, the diameter of ZnO particles is tunable from 18 nm to 436 nm. For all solvent compositions, a high homogeneity of nanoparticles could be achieved if high flow rates were applied. The high homogeneity is attributed to the fast mixing in the static micro-mixer and by the fast heat transfer inside the small droplets of reaction mixture caused by the flow-induced fast segment-internal convection. UV/vis absorption spectra confirm the change of particle quality in case of increasing water contents. In particular, at the water content below 50 v%, ZnO nanoparticles with homogeneous size distribution were obtained. Therefore, the segmented flow synthesis is a useful technology to prepare ZnO nanoparticles and should be an interesting option to prepare other metal or metal oxide nanosized powders.

Acknowledgements

We would like to thank Dr. G.A. Groß, Prof. E. Rädlein, Dr. P. Denner and Dr. U. Ritter for scientific discussions. The technical support of Mrs. F. Möller and Mr. S. Schneider is gratefully acknowledged. We also appreciate Mr. J. Schawohl for XRD measurement, Dr. H. Romanus for TEM measurement and Mrs. D. Raab for TG–DTA analysis.

References

[1] S. Choopun, A. Tubtimtae, T. Santhaveesuk, S. Nilphai, E. Wongrat, N. Hongsith, Zinc oxide nanostructures for applications as ethanol sensors and dye-sensitized solar cells, Applied Surface Science 256 (2009) 998–1002.
[2] J. Tornow, K. Schwarzburg, Transient electrical response of dye-sensitized ZnO nanorod solar cells, Journal of Physical Chemistry C 111 (2007) 8692–8698.
[3] R. Zhang, S. Kumar, S. Zou, L.L. Kerr, High-density vertically aligned ZnO rods with a multistage terrace structure and their improved solar cell efficiency, Crystal Growth and Design 8 (2007) 381–383.
[4] T. Sun, J. Qiu, C. Liang, Controllable fabrication and photocatalytic activity of ZnO nanobelt arrays, The Journal of Physical Chemistry C 112 (2007) 715–721.
[5] H. Wang, G. Li, L. Jia, G. Wang, C. Tang, Controllable preferential-etching synthesis and photocatalytic activity of porous ZnO nanotubes, The Journal of Physical Chemistry C 112 (2008) 11738–11743.
[6] F. Li, Y. Jiang, L. Hu, L. Liu, Z. Li, X. Huang, Structural and luminescent properties of ZnO nanorods and ZnO/ZnS nanocomposites, Journal of Alloys and Compounds 474 (2009) 531–535.
[7] J. Zhang, H. Feng, W. Hao, T. Wang, Luminescent properties of ZnO sol and film doped with Tb3+ ion, Materials Science and Engineering: A 425 (2006) 346–348.
[8] D. Calestani, M. Zha, R. Mosca, A. Zappettini, M.C. Carotta, V. Di Natale, L. Zanotti, Growth of ZnO tetrapods for nanostructure-based gas sensors, Sensors and Actuators B-Chemical 144 (2010) 472–478.
[9] S.K. Gupta, A. Joshi, M. Kaur, Development of gas sensors using ZnO nanostructures, Journal of Chemical Sciences 122 (2010) 57–62.
[10] F.T. Liu, S.F. Gao, S.K. Pei, S.C. Tseng, C.H.J. Liu, ZnO nanorod gas sensor for NO_2 detection, Journal of the Taiwan Institute of Chemical Engineers 40 (2009) 528–532.
[11] O. Akhavan, M. Mehrabian, K. Mirabbaszadeh, R. Azimirad, Hydrothermal synthesis of ZnO nanorod arrays for photocatalytic inactivation of bacteria, Journal of Physics D – Applied Physics 42 (2009).
[12] L. Li, H.Q. Yang, H. Zhao, J. Yu, J.H. Ma, L.J. An, X.W. Wang, Hydrothermal synthesis and gas sensing properties of single-crystalline ultralong ZnO nanowires, Applied Physics A – Materials Science and Processing 98 (2010) 635–641.
[13] K.J. Chen, F.Y. Hung, S.J. Chang, Z.S. Hu, The crystallized mechanism and optical properties of sol–gel synthesized ZnO nanowires, Journal of the Electrochemical Society 157 (2010) H241–H245.
[14] C.H. Chia, Y.J. Lai, T.C. Han, J.W. Chiou, Y.M. Hu, W.C. Chou, High-excitation effect on photoluminescence of sol–gel ZnO nanopowder, Applied Physics Letters 96 (2010).
[15] N.V. Kaneva, G.G. Yordanov, C.D. Dushkin, Photocatalytic action of ZnO thin films prepared by the sol–gel method, Reaction Kinetics and Catalysis Letters 98 (2009) 259–263.
[16] S. Labuayai, V. Promarak, S. Maensiri, Synthesis and optical properties of nanocrystalline ZnO powders prepared by a direct thermal decomposition route, Applied Physics A – Materials Science and Processing 94 (2009) 755–761.
[17] C.C. Lin, Y.Y. Li, Synthesis of ZnO nanowires by thermal decomposition of zinc acetate dihydrate, Materials Chemistry and Physics 113 (2009) 334–337.
[18] S. Cho, D.S. Shim, S.H. Jung, E. Oh, B.R. Lee, K.H. Lee, Fabrication of ZnO nanoneedle arrays by direct microwave irradiation, Materials Letters 63 (2009) 739–741.
[19] X.R. Kong, Y.Q. Duan, P. Peng, C. Qiu, L.Y. Wu, L. Liu, W.J. Zheng, A novel route to prepare ZnO nanotubes by using microwave irradiation method, Chemistry Letters 36 (2007) 428–429.
[20] N. Sakamoto, S. Ishizuka, N. Wakiya, H. Suzuki, Shape controlled ZnO nanoparticle prepared by microwave irradiation method, Journal of the Ceramic Society of Japan 117 (2009) 961–963.
[21] F. Falyouni, L. Benmamas, C. Thiandoume, J. Barjon, A. Lusson, P. Galtier, V. Sallet, Metal organic chemical vapor deposition growth and luminescence of ZnO micro- and nanowires, Journal of Vacuum Science and Technology B 27 (2009) 1662–1666.
[22] N. Zhang, R. Yi, R.R. Shi, G.H. Gao, G. Chen, X.H. Liu, Novel rose-like ZnO nanoflowers synthesized by chemical vapor deposition, Materials Letters 63 (2009) 496–499.
[23] S.Y. Han, Y.J. Chang, D.H. Lee, S.O. Ryu, T.J. Lee, C.H. Chang, Chemical nanoparticle deposition of transparent ZnO thin films, Electrochemical and Solid-State Letters 10 (2007) K1–K5.
[24] J.Y. Jung, N.-K. Park, S.-Y. Han, G.B. Han, T.J. Lee, S.O. Ryu, C.-H. Chang, The growth of the flower-like ZnO structure using a continuous flow microreactor, Current Applied Physics 8 (2008) 720–724.
[25] N. Bouropoulos, I. Tsiaoussis, P. Poulopoulos, P. Roditis, S. Baskoutas, ZnO controllable sized quantum dots produced by polyol method: an experimental and theoretical study, Materials Letters 62 (2008) 3533–3535.

[26] S. Lee, S. Jeong, D. Kim, S. Hwang, M. Jeon, J. Moon, ZnO nanoparticles with controlled shapes and sizes prepared using a simple polyol synthesis, Superlattices and Microstructures 43 (2008) 330–339.
[27] C.G. Li, Y. Zhao, L. Wang, G.H. Li, Z. Shi, S.H. Feng, Polyol-mediated synthesis of highly water-soluble ZnO colloidal nanocrystal clusters, European Journal of Inorganic Chemistry (2010) 217–220.
[28] X.S. Tang, E.S.G. Choo, L. Li, J. Ding, J.M. Xue, One-pot synthesis of water-stable ZnO nanoparticles via a polyol hydrolysis route and their cell labeling applications, Langmuir 25 (2009) 5271–5275.
[29] C. Chen, L. Wang, G.H. Jiang, J.F. Zhou, X. Chen, H.J. Yu, Q. Yang, Study on the synthesis of silver nanowires with adjustable diameters through the polyol process, Nanotechnology 17 (2006) 3933–3938.
[30] Y.H. Lee, D.W. Kim, S.I. Shin, S.G. Oh, Preparation of Au colloids by polyol process using NaHCO3 as a buffering agent, Materials Chemistry and Physics 100 (2006) 85–91.
[31] Y.G. Sun, Y.N. Xia, Large-scale synthesis of uniform silver nanowires through a soft, self-seeding, polyol process, Advanced Materials 14 (2002) 833–837.
[32] C Feldmann, Polyol-mediated synthesis of nanoscale functional materials, Advanced Functional Materials 13 (2003) 101–107.
[33] T. Yamamoto, Y. Wada, H.B. Yin, T. Sakata, H. Mori, S. Yanagida, Microwave-driven polyol method for preparation of TiO_2 nanocrystallites, Chemistry Letters (2002) 964–965.
[34] M. Donnet, N. Jongen, J. Lemaitre, P. Bowen, New morphology of calcium oxalate trihydrate precipitated in a segmented flow tubular reactor, Journal of Materials Science Letters 19 (2000) 749–750.
[35] A. Grodrian, J. Metze, T. Henkel, K. Martin, M. Roth, J.M. Köhler, Segmented flow generation by chip reactors for highly parallelized cell cultivation, Biosensors and Bioelectronics 19 (2004) 1421–1428.
[36] N. Jongen, M. Donnet, P. Bowen, J. Lemaitre, H. Hofmann, R. Schenk, C. Hofmann, M. Aoun-Habbache, S. Guillemet-Fritsch, J. Sarrias, A. Rousset, M. Viviani, M.T. Buscaglia, V. Buscaglia, P. Nanni, A. Testino, J.R. Herguijuela, Development of a continuous segmented flow tubular reactor and the "scale-out" concept – in search of perfect powders, Chemical Engineering and Technology 26 (2003) 303–305.
[37] J.M. Köhler, T. Kirner, Nanoliter segment formation in micro fluid devices for chemical and biological micro serial flow processes in dependence on flow rate and viscosity, Sensors and Actuators a – Physical 119 (2005) 19–27.
[38] H. Song, J.D. Tice, R.F. Ismagilov, A microfluidic system for controlling reaction networks in time, Angewandte Chemie – International Edition 42 (2003) 768–772.
[39] R. Vacassy, J. Lemaitre, H. Hofmann, J.H. Gerlings, Calcium carbonate precipitation using new segmented flow tubular reactor, AIChE Journal 46 (2000) 1241–1252.
[40] A. Funfak, A. Brosing, M. Brand, J.M. Köhler, Micro fluid segment technique for screening and development studies on *Danio rerio* embryos, Lab on a Chip 7 (2007) 1132–1138.
[41] K. Martin, T. Henkel, V. Baier, A. Grodrian, T. Schön, M. Roth, J.M. Köhler, J. Metze, Generation of larger numbers of separated microbial populations by cultivation in segmented-flow microdevices, Lab on a Chip 3 (2003) 202–207.
[42] T. Kirner, J. Albert, M. Günther, G. Mayer, K. Reinhäckel, J.M. Köhler, Static micromixers for modular chip reactor arrangements in two-step reactions and photochemical activated processes, Chemical Engineering Journal 101 (2004) 65–74.
[43] J.D. Tice, H. Song, A.D. Lyon, R.F. Ismagilov, Formation of droplets and mixing in multiphase microfluidics at low values of the Reynolds and the capillary numbers, Langmuir 19 (2003) 9127–9133.
[44] K.F. Jensen, Microreaction engineering – is small better? Chemical Engineering Science 56 (2001) 293–303.
[45] H. Song, D.L. Chen, R.F. Ismagilov, Reactions in droplets in microflulidic channels, Angewandte Chemie – International Edition 45 (2006) 7336–7356.
[46] Z. Hu, D.J. Escamilla Ramirez, B.E. Heredia Cervera, G. Oskam, P.C. Searson, Synthesis of ZnO nanoparticles in 2-propanol by reaction with water, The Journal of Physical Chemistry B 109 (2005) 11209–11214.
[47] L. Brus, Electronic wave functions in semiconductor clusters: experiment and theory, The Journal of Physical Chemistry 90 (1986) 2555–2560.
[48] N.S. Pesika, K.J. Stebe, P.C. Searson, Relationship between absorbance spectra and particle size distributions for quantum-sized nanocrystals, The Journal of Physical Chemistry B 107 (2003) 10412–10415.
[49] A. Dakhlaoui, M. Jendoubi, L.S. Smiri, A. Kanaev, N. Jouini, Synthesis, characterization and optical properties of ZnO nanoparticles with controlled size and morphology, Journal of Crystal Growth 311 (2009) 3989–3996.
[50] B.G Wang, E.W. Shi, W.Z. Zhong, Understanding and controlling the morphology of ZnO crystallites under hydrothermal conditions, Crystal Research and Technology 32 (1997) 659–667.